

RUNX transcription factors potentially control E-selectin expression in the bone marrow vascular niche in mice

Ken Morita,^{1,*} Chieko Tokushige,^{1,*} Shintaro Maeda,¹ Hiroki Kiyose,¹ Mina Noura,¹ Atsushi Iwai,² Maya Yamada,¹ Gengo Kashiwazaki,³ Junichi Taniguchi,³ Toshikazu Bando,³ Masahiro Hirata,⁴ Tatsuki R. Kataoka,⁴ Tatsutoshi Nakahata,⁵ Souichi Adachi,^{1,2} Hiroshi Sugiyama,³ and Yasuhiko Kamikubo¹

¹Department of Human Health Sciences, Graduate School of Medicine, ²Department of Pediatrics, Graduate School of Medicine, and ³Department of Chemistry, Graduate School of Science, Kyoto University, Kyoto, Japan; ⁴Department of Diagnostic Pathology, Kyoto University Hospital, Kyoto, Japan; and ⁵Drug Discovery Technology Development Office, Center for iPS Cell Research and Application, Kyoto University, Kyoto, Japan

Key Points

- RUNX transcription factors potentially transactivate *E-selectin* expression in the vascular niche.
- RUNX inhibitor disrupts engraftment of AML cells in the bone marrow, possibly by attenuating E-selectin expression.

Although the function of Runt-related (RUNX) transcription factors has been well characterized in leukemogenesis and regarded as an ideal target in antileukemia strategies, the effect of RUNX-inhibition therapy on bone marrow niche cells and its impact on the engraftment of acute myeloid leukemia (AML) cells have largely been unknown. Here, we provide evidence suggesting the possible involvement of RUNX transcription factors in the transactivation of *E-selectin*, a member of selectin family of cell adhesion molecules, on the vascular endothelial cells of the mice bone marrow niche. In our experiments, gene switch-mediated silencing of RUNX downregulated E-selectin expression in the vascular niche and negatively controlled the engraftment of AML cells in the bone marrow, extending the overall survival of leukemic mice. Our work identified the novel role of RUNX family genes in the vascular niche and showed that the vascular niche, a home for AML cells, could be strategically targeted with RUNX-silencing antileukemia therapies. Considering the excellent efficacy of RUNX-inhibition therapy on AML cells themselves as we have previously reported, this strategy potentially targets AML cells both directly and indirectly, thus providing a better chance of cure for poor-prognostic AML patients.

Introduction

While the leukemogenic role of Runt-related (RUNX) transcription factors has been intensively studied and well described in acute myeloid leukemia (AML),¹⁻⁶ little is known about the effect of *RUNX* inhibition on the microenvironment surrounding tumor cells in vivo. Leukemic stem cells reside in the distinct regions within this microenvironment called niches. These niches maintain the principle properties of leukemic stem cells, protect them from the immune surveillance, and facilitate their oncogenic potential.⁷ In the bone marrow, the vascular niche and the osteoblastic niche are the 2 major components of this microenvironment. Although discovered later than osteoblastic niche, vascular niche is now regarded as an alternative indispensable niche regulating hematopoietic stem cells (HSCs).^{8,9} Endothelial selectins are cell adhesion molecules expressed in the vascular niche. Selectins are a family of 3 cell adhesion molecules (E-, L- and P-selectins) with well-characterized roles in leukocyte homing. Among them, the crucial role of E-selectin as a component of the vascular niche has been recently discovered, and inhibition of E-selectin is reported to enhance chemoresistance of normal HSCs and accelerate blood neutrophil recovery after chemotherapeutic treatment.¹⁰ Previous reports suggest that the survival of AML blasts is enhanced by their adhesion to the vascular niche via E-selectin.^{11,12} Although these

findings underpin the rationale for using an E-selectin–targeting strategy in antileukemia treatment, precise mechanisms in transcriptional regulation of *E-selectin* have remained mostly unknown. Here, we address this issue and elaborate to clarify the role of RUNX transcription factors in the vascular niche in AML.

Methods

Cell lines

Embryonic kidney–derived HEK293T cells were purchased from the Japanese Collection of Research Bioresources. AML-derived MV4-11 cells and bone osteosarcoma–derived HOS cells were obtained from the American Type Culture Collection. HEK293T and HOS cells were maintained in Dulbecco's modified Eagle's medium supplemented with 10% heat-inactivated fetal bovine serum (FBS) and 1% penicillin-streptomycin at 37°C, 5% CO₂. MV4-11 cells were cultured in RPMI 1640 medium with 10% FBS and 1% penicillin-streptomycin at 37°C, 5% CO₂. Human umbilical vein endothelial cells (HUVECs) were purchased from PromoCell and maintained in endothelial cell growth medium 2 (PromoCell) at 37°C, 5% CO₂.

ChIP-qPCR

Chromatin immunoprecipitation (ChIP) was performed using the SimpleChIP Plus Enzymatic Chromatin IP Kit (Cell Signaling Technology) according to the manufacturer's instructions. In brief, cells were cross-linked in 1% formaldehyde in PBS for 10 minutes at room temperature. After glycine quenching, cell pellets were collected and lysed and then subjected to sonication (Q55 sonicator system, QSONICA). The supernatant was diluted with the same sonication buffer and processed for immunoprecipitation with the following antibodies at 4°C overnight: anti-RUNX1 (ab23980, Abcam), anti-RUNX2 (D1H7 rabbit monoclonal antibody 8486, Cell Signaling Technology), and anti-RUNX3 (ab11905, Abcam). The beads were then washed, and DNA was reverse cross-linked and purified. Following ChIP, DNA was quantified by quantitative polymerase chain reaction (qPCR) using the standard procedures for 7500 Real-Time PCR System (Applied Biosystems). Primers used for ChIP-qPCR are listed in supplemental Table 1.

Real-time qPCR

Total RNA was isolated using the RNeasy mini kit (Qiagen) and reverse transcribed with a reverse script kit (Toyobo) to generate complementary DNA. Real-time qPCR was carried out with the 7500 Real-Time PCR System (Applied Biosystems) according to the manufacturer's instructions. The results were normalized to *GAPDH* levels. Relative expression levels were calculated using the $2^{-\Delta\Delta C_t}$ method. Primers used for real-time qPCR are listed in supplemental Table 2.

Small interfering RNA interference

A specific short hairpin RNA (shRNA) targeting human *RUNX1* was designed and subcloned into pENTR4-H1tetOx1, CS-RfA-ETBsd, CS-RfA-ETV, and CS-RfA-ETR vectors (RIKEN BioResource Center). Nontargeting control shRNA was designed against *luciferase* (sh_*Luc.*). Target sequences are provided in supplemental Table 3.

Production and transduction of lentivirus

Production and transduction of lentivirus was conducted as previously described.¹³ For the production of lentivirus, HEK293T cells were transiently cotransfected with lentivirus vectors such as

psPAX2 and pMD2.G with polyethylenimine (Sigma-Aldrich). Forty-eight hours after transfection, viral supernatants were collected and immediately used for infection, and then successfully transduced cells were sorted by flow cytometry (Aria III, BD Biosciences).

Homing and engraftment assay

For the homing and engraftment assay, C57BL/6 mice were either preconditioned by andrographolide (given 3 times per week, intraperitoneally [IP]), A 205804 (given 3 times per week, orally), or Chb-M' (given 3 times per week, IV) for 2 weeks. Twenty-four hours after the last administration, 1×10^6 GFP+ AML cells from MLL-ENL mice were injected IV through the tail veins. Twenty-four hours after transplantation, mice were properly euthanized, and the frequency of GFP+ cells in the femur bone marrow and spleen were determined using a BD FACS Canto II flow cytometer.

Statistical analysis

Differences between control and experimental groups were assessed using a 2-tailed unpaired Student *t* test and declared statistically significant if $P < .05$. Equality of variances in 2 populations was calculated with the F test. Results are presented as mean \pm standard error of the mean (SEM) values obtained from 3 independent experiments. In transplantation experiments, animals were randomly allocated to each experimental group, and the treatments were given with blinding. The overall survival of mice is shown in a Kaplan-Meier curve. Survival between the indicated groups was compared using the log-rank test. To measure the correlation between mRNA or protein expression, Spearman's rank correlation coefficient was used.

Study approval

All animal studies were properly conducted in accordance with the Regulation on Animal Experimentation at Kyoto University, based on International Guiding Principles for Biomedical Research Involving Animals. All procedures employed in this study were approved by the Kyoto University Animal Experimentation Committee (permit Med Kyo 14332).

Synthesis of PI polyamides

Synthesis of Chb-M' was conducted as previously reported.⁶ Briefly, pyrrole-imidazole (PI) polyamide supported by oxime resin was prepared in a stepwise reaction using the Fmoc solid-phase protocol. The product with oxime resin was cleaved with *N,N*-dimethyl-1,3-propane diamine (1.0 mL) at 45°C for 3 hours. The residue was dissolved in the minimum amount of dichloromethane and washed with diethyl ether to yield 59.6 mg. To the crude compound (59.6 mg, 48.1 μ mol), a solution of chlorambucil (32.6 mg, 107 μ mol), PyBOP (benzotriazole-1-yl-oxy-tris-pyrrolidino-phosphonium hexafluorophosphate) (101 mg, 195 μ mol), and *N,N*-diisopropylethylamine (100 μ L, 581 μ mol) in *N,N*-dimethylformamide (300 μ L) was added. The reaction mixture was incubated for 1.5 hours at room temperature, washed with diethyl ether and *N,N*-dimethylformamide 3 times, and dried in vacuo. The crude product was purified by reversed-phase flash column chromatography (water with 0.1% trifluoroacetic acid/MeCN). After lyophilization, product was obtained (30.2 mg, 19.8 μ mol). Machine-assisted polyamide syntheses were performed on a PSSM-8 (Shimadzu) system with computer-assisted operation. Flash column purifications were performed by a CombiFlash Rf (Teledyne Isco) with C18 RediSep Rf Flash Column. Electrospray ionization time-of-flight

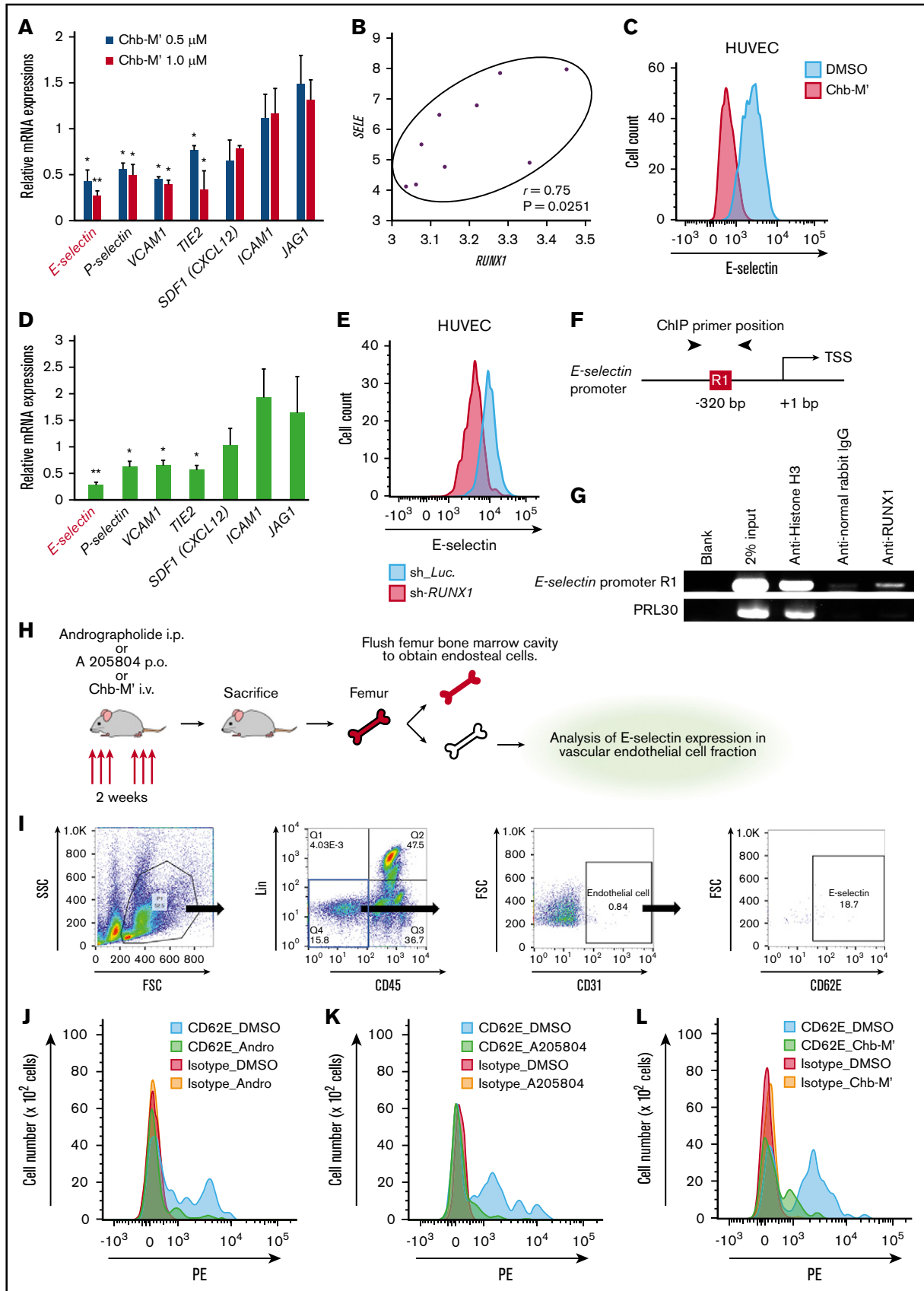


Figure 1.

mass spectrometry was performed on a Bio-TOF II (Bruker Daltonics) mass spectrometer using a positive ionization mode, and proton nuclear magnetic resonance spectra were recorded with a JEOL JNM ECA-600 spectrometer operating at 600 MHz and in parts per million downfield relative to tetramethylsilane, which was used as an internal standard to verify the quality of synthesized PI polyamides.

E-selectin static adhesion assay

The E-selectin static adhesion assay was conducted as previously described, with minor modifications.¹⁰ Briefly, 96-well plates were coated with purified recombinant mouse VCAM-1 or E-selectin-human IgG1 (hulgG1)-Fc fusion proteins (R&D Systems) at the indicated concentrations in 40 μ l of 20 mM Tris-buffered saline (pH 7.4) with 1 mM CaCl₂ at 4°C for 16 hours and then washed and blocked with 100 μ l IMDM + 1% BSA at room temperature for 1 hour. c-KIT positive fraction of mice AML cells with MLL-ENL were sorted and 5 \times 10³ cells were seeded for each well. After gentle sedimentation by centrifugation (4°C, 1500 rpm, 10 min), cells were left in contact with the coated surface for 30 min at 4°C, washed 4 times with PBS plus 3% FBS to remove nonadhesive cells, and the percentage of adherent cells was quantified with Cell Count Reagent SF (Nacalai Tesque) and a multiplate reader (Infinite200 PRO, Tecan).

Flow cytometry

MLL-ENL fusion gene was retrovirally transduced to c-kit⁺ primary mice bone marrow cells to obtain AML cells from immortalized mice. Detection or isolation of c-kit⁺ fraction from mice normal or leukemic bone cells retrovirally transduced with MLL-ENL harboring GFP immunofluorescent color marker expression and human cell lines transduced with shRNA lentivirus vectors harboring Venus expressions were performed using FACS Aria III (BD) cell sorter. To obtain endothelial vascular niche cells, mice femurs were collected after proper euthanasia and flushed into ice-cold PBS plus 2% newborn calf serum for the isolation of bone marrow cells. The empty femurs were flushed twice more in PBS then flushed with 1 mg/mL collagenase 1 every 5 min at 37°C for 30 minutes to

dislodge endosteal cells, which were then used for flow cytometry. The following antibodies were used to identify E-selectin expression in mouse endothelial cells: fluorescein isothiocyanate anti-mouse LIN (CD3/Gr-1/CD11b/CD45R(B220)/Ter-119, Pacific Blue anti-mouse CD45 (30-F11), allophycocyanin anti-mouse CD31 (390) (BioLegend), phycoerythrin (PE) rat anti-mouse CD62E (10E9.6) (BD Pharmingen), and PE rat anti-mouse isotype control (PE rat immunoglobulin G2a [IgG2a], κ isotype control, clone R35-95) (BD Biosciences). E-selectin expressions in HUVEC was detected by anti-human CD62E (E-selectin) PE (P2H3) antibody (eBioscience).

Mice

C57BL/6J mice were purchased from CLEA Japan. NOD/Shi-scid, IL-2R γ KO (NOG) mice were purchased from the Central Institute for Experimental Animals (Japan). Littermates were used as controls in all experiments.

Transplantation assay

For transplantation assay, mice were either preconditioned with Chb-M' 320 μ g/kg body weight twice per week IV or control dimethyl sulfoxide (DMSO) (IV) for 2 weeks. Twenty-four hours after the last administration, 1 \times 10⁶ MV4-11 cells were injected IV through the tail vein to NOG mice. Seven days after transplantation, mice were treated with either Chb-M' 320 μ g/kg body weight twice per week IV or control DMSO until they showed physical signs of leukemia development.

Results and discussion

To investigate the effect of *RUNX1* inhibition on the endothelial vascular niche cells, we first screened the expression of representative surface molecules in HUVECs treated with either the selective *RUNX* inhibitor Chb-M'⁶ or control DMSO. As shown in Figure 1A, Chb-M' treatment significantly suppressed the expressions of *E-selectin*, *P-selectin*, *VCAM1*, and *TIE2*. Among them, we focused on *E-selectin* not only because it was the most profoundly attenuated molecule in our screen but also because it has recently been recognized as a vital component of vascular niche and

Figure 1. Inhibition of RUNX1 attenuates the E-selectin expression. (A) Relative expression of *E-selectin*, *P-selectin*, *VCAM1*, *TIE2*, *SDF1* (*CXCL12*), *ICAM1*, and *JAG1* was determined in HUVECs treated with control DMSO or Chb-M' at 0.5 μ M or 1.0 μ M. Twenty-four hours after treatment, total RNA was prepared and processed for real-time qPCR analysis. Values are normalized to those of DMSO-treated cells (n = 3). (B) Correlation between the expression levels of *RUNX1* and *E-selectin* in HUVEC cell lines established from 9 different umbilical cords (n = 9). Values represent array signal intensities. P values were determined using Spearman's correlation. (C) Surface expressions of E-selectin were determined in HUVEC treated either by control DMSO or Chb-M' at 1 μ M. Forty-eight hours after treatment, cells were harvested and stained for flow cytometric analysis. (D) Relative expression of *E-selectin*, *P-selectin*, *VCAM1*, *TIE2*, *SDF1* (*CXCL12*), *ICAM1*, and *JAG1* was determined in HUVECs transduced with control (sh_*Luc*) or *RUNX1* shRNA (sh_*RUNX1*) in the presence of 3 μ M doxycycline. Twenty-four hours after treatment, total RNA was prepared and processed for real-time RT-PCR analysis. Values are normalized to that of control cells (n = 3). (E) Surface expression of E-selectin was determined in HUVECs transduced with sh_*Luc* or sh_*RUNX1* in the presence of 3 μ M doxycycline. Forty-eight hours after treatment, cells were harvested and stained for flow cytometric analysis. (F) Schematic illustration showing the proximal regulatory region (–600 bp to +200 bp of the transcription start site) of *E-selectin*. (G) ChIP analysis in HUVECs using anti-*RUNX1* antibody, an isotope-matched control IgG, and anti-histone H3 antibody. ChIP products were subjected to PCR-based amplification with the indicated primer sets (supplemental Table 1), using RPL30 as a negative control. (H) Schematic representation of the treatment and analysis schedule in C57BL/6 mice. Mice were treated with andrographolide (25 mg/kg body weight, 3 times/week, IP), A 205804 (10 mg/kg body weight, 3 times/week, orally [p.o.]), or Chb-M' (320 μ g/kg body weight, 3 times/week, IV) for 2 weeks. After treatment, mice were sacrificed, and endosteal cells were dislodged from the femurs for further analysis. (I) Representative flow cytometry analysis identifying vascular niche cells in the endosteal cells obtained in panel H. Expression of E-selectin was determined in the indicated endothelial cells (Lin[–]CD45[–]CD31⁺). (J) Representative flow cytometry analysis of E-selectin expression in endothelial cells in mice treated with control DMSO or andrographolide. (K) Representative flow cytometry analysis of E-selectin expression in endothelial cells in mice treated with control DMSO or A 205804. (L) Representative flow cytometry analysis of E-selectin expression in endothelial cells in mice treated with control DMSO or Chb-M'. Data are presented as mean \pm SEM. *P < .05, **P < .01 (2-tailed Student t test). FSC, forward scatter; SSC, side scatter.

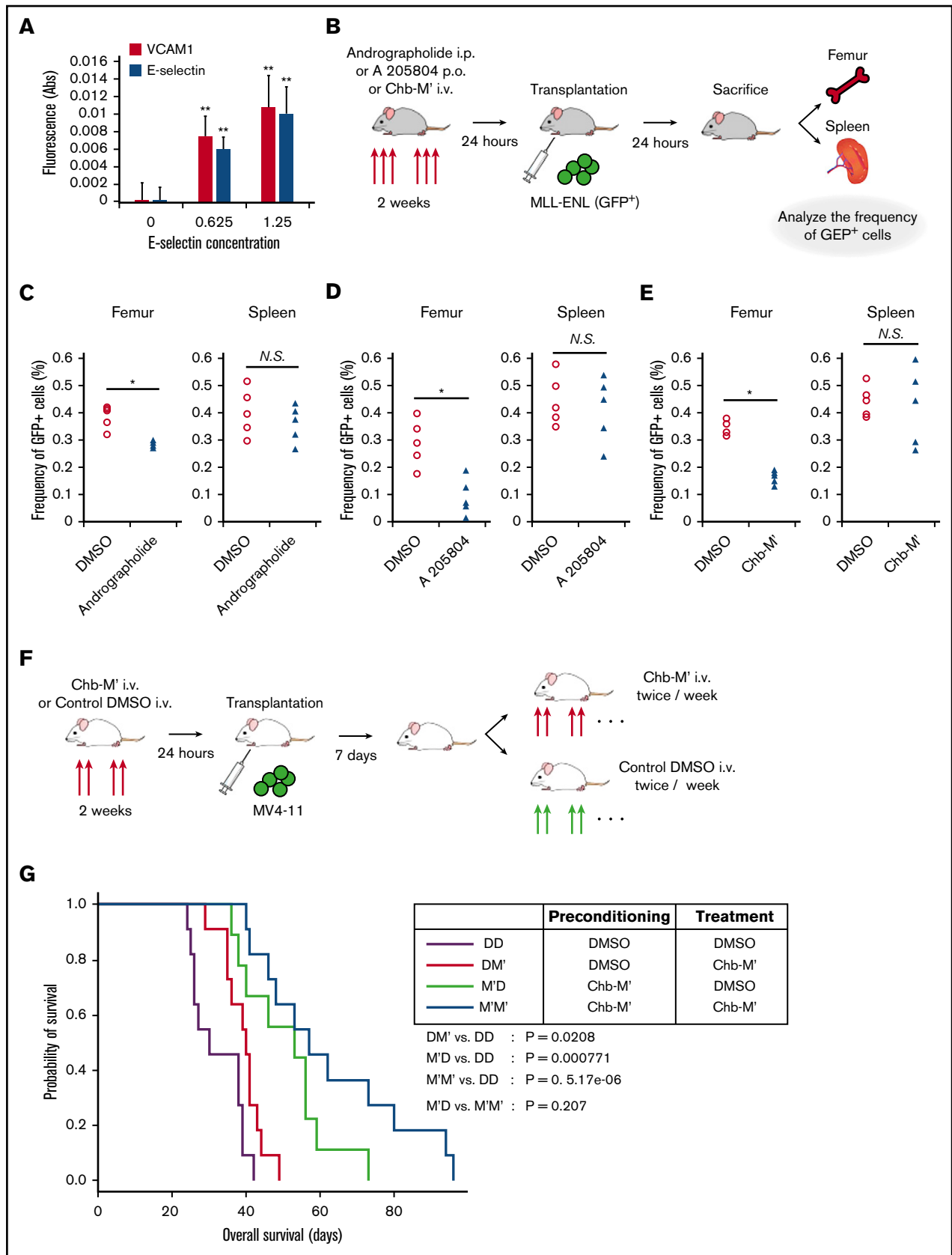


Figure 2. RUNX1-inhibition potently inhibits the homing of AML cells to the vascular niche. (A) Cumulative result of the E-selectin static adhesion assay. MLL-ENL⁺ mouse leukemic cells were seeded to the E-selectin-coated plate at the indicated concentrations, and adhesive cells were counted using a fluorometer (n = 4). (B) Schematic

fundamentally involved in the housing of HSCs.¹⁰ As shown in Figure 1B, *RUNX1* and *E-selectin* expression is indeed positively correlated among HUVEC cell lines with significance. In addition, the surface expression of E-selectin was decreased upon Chb-M' treatment with significance in HUVECs (Figure 1C). To extend the robustness of our findings, we genetically attenuated the expression of *RUNX1* in HUVECs with doxycycline-inducible shRNA. As expected, the expression of E-selectin was tightly and most profoundly downregulated both at the transcript level and the surface expression level upon *RUNX1* silencing (Figure 1D-E). On the other hand, additive expression of *RUNX1* in HUVECs resulted in the upregulation of *E-selectin*, of which finding was consistent with those obtained in *RUNX1* knockdown experiments (supplemental Figure 1A-B). Of note, neither Chb-M'-treatment nor shRNA-mediated *RUNX1* knockdown resulted in significant change in the expression of niche-associated surface molecules in AML-derived MV4-11 cells (supplemental Figure 2A-B). In addition, neither Chb-M' treatment nor *RUNX1* knockdown resulted in a significant change in the expression of osteoblastic niche components in osteosarcoma-derived HOS cells (supplemental Figure 3A-B). These results suggest that *RUNX1* potentially and primordially be involved in the regulation of E-selectin in the endothelial vascular niche cells. Close inspection of the *E-selectin* promoter revealed the canonical *RUNX* binding sequence of 5'-TGTGGT-3' in 320 bp upstream of the transcription start site (Figure 1F). As shown in Figure 1G, we have confirmed the actual binding of *RUNX1* in this site by ChIP assay. Activity of *E-selectin* promoter was increased in the additional *RUNX1* expression while the modified *E-selectin* promoter which lacks this 5'-TGTGGT-3' site dramatically decreased its luciferase reporter activity, confirming the vital role of *RUNX1* in *E-selectin* transactivation (supplemental Figure 4A-C). Because all *RUNX* family members recognize these consensus sequences, we next addressed the possible involvement of other *RUNX* family members in *E-selectin* regulation. Interestingly, *RUNX2* knockdown, but not *RUNX3* knockdown, showed attenuation of *E-selectin* expression in HUVECs (supplemental Figure 5A-B). The ChIP assay also revealed the binding of *RUNX2* to the *E-selectin* promoter, but it failed to show the binding of *RUNX3* (supplemental Figure 6A-B). These results indicate the possible involvement of *RUNX2* and *RUNX1* in *E-selectin* transactivation.

To further investigate the role of *RUNX* transcription factors in the niche, we next examined the effect of *Runx* attenuation on E-selectin expression in endothelial vascular niche cells in mice (Figure 1H). To appropriately set the gates in fluorescence-activating cell sorter (FACS) analysis, we first confirmed that the expression of endothelial markers such as *Sca-1* and *VE-cadherin*

were consistently higher in CD31⁺ cells relative to CD31⁻ cells (supplemental Figure 7A-B). Treating C56BL/6 mice either with the previously validated E-selectin inhibitors andrographolide¹⁴ and A 205804¹⁵ or with the *Runx* inhibitor Chb-M' for 2 weeks indeed efficiently decreased the expression of E-selectin on the endothelial vascular niche cells (Figure 1I-L). We next retrovirally transduced MLL-ENL to c-kit⁺ mice bone marrow cells and obtained leukemic cells. Using these mouse leukemic cells, we investigated the effect of *Runx* inhibition therapy on the homing ability of leukemia cells to their bone marrow niche. Firstly, we conducted in vitro static assay to examine the E-selectin-mediated adhesion of AML cells. As shown in Figure 2A, the number of AML cells attached to the plate was proportional to the coated E-selectin concentrations. We next treated mice with andrographolide, A 205804, or Chb-M' for 2 weeks followed by transplantation of MLL-ENL⁺ leukemic cells (Figure 2B). To minimize unwanted direct antitumor effect of the drugs on the transplanted AML cells, we used a 24-hour washout period before transplantation. As shown in Figure 2C-E, these treatments significantly decreased the number of homed leukemic cells in the bone marrow compared with the vehicle-treated mice, underscoring the importance of E-selectin in the engraftment of AML cells in the vascular niche. Intriguingly, E-selectin was reported to exclusively express in the endothelial vascular niche in the bone marrow, whereas no expression was detected in spleen cells.¹⁰ In our homing experiments, we indeed observed no change in the number of homed leukemic cells in the spleens of mice treated with Chb-M', andrographolide, or A 205804, showing that the inhibition of *Runx*-mediated E-selectin regulation specifically disrupts the homing of leukemia cells in the bone marrow (Figure 2C-E). Consistent with these observations, conditioning bone marrow vascular niche with Chb-M' before transplantation of leukemic cells significantly prolonged the overall survival periods of AML mice (Figure 2F-G). Although we acknowledge that pharmacologic inhibition of *RUNX* or E-selectin are not fully specific and our findings should further be examined in genetically engineered mice to rule out the involvement of other unknown mechanisms, our results indicate that *RUNX*-silencing drugs such as Chb-M' not only directly control the growth of AML cells themselves⁶ but also indirectly enhance their antileukemic potential, possibly by attenuating E-selectin expression in the bone marrow vascular niche. Because we observed consistently higher numbers of circulating transplanted AML cells in the peripheral blood of Chb-M'-pretreated mice relative to control mice, these drugs could potentially bring leukemic stem-like cells out from deep in the bone marrow niche to the peripheral bloodstream and expose these primordial leukemia cells to chemotherapeutic drugs at much higher concentrations (supplemental Figure 8A).

Figure 2. (continued) representation of the treatment and analysis schedule in mice. C57BL/6 mice were treated with andrographolide (25 mg/kg body weight, 3 times/week, IP), A 205804 (10 mg/kg body weight, 3 times/week, orally), or Chb-M' (320 μg/kg body weight, 3 times/week, IV) for 2 weeks. Twenty-four hours after the last treatment, mice were transplanted with 1×10^6 MLL-ENL⁺ leukemic cells marked with GFP fluorescence. After another 24 hours, when all mice were sacrificed for flow cytometric analysis, the frequency of GFP⁺ cells in the femur and spleen was determined. (C) Frequency of GFP⁺ leukemic cells in the femur and the spleen in mice treated with control DMSO or andrographolide (n = 5). (D) Frequency of GFP⁺ leukemic cells in the femur and spleen in mice treated with control DMSO or A 205804 (n = 5). (E) Frequency of GFP⁺ leukemic cells in the femur and spleen in mice treated with control DMSO or Chb-M' (n = 5). (F) Schematic representation of the treatment and analysis schedule in mice. NOG mice were preconditioned with Chb-M' (320 μg/kg body weight, 3 times/week, IV) or control DMSO for 2 weeks. Twenty-four hours after the last administration, mice were transplanted with 1×10^6 MV4-11 cells. Seven days later, when treatment with Chb-M' (320 μg/kg body weight, twice per week, IV) or control DMSO began, we looked for signs of leukemia development. (G) Overall survival of mice transplanted with MV4-11 cells followed by treatment with Chb-M' or control DMSO as in panel A (DMSO, DMSO [DD]: n = 11; Chb-M', DMSO [M'D]: n = 9; DMSO, Chb-M' [DM]: n = 11; Chb-M', Chb-M' [M'M]: n = 11). Data represent mean ± SEM. P values were determined using a log-rank (Mantel-Cox) test. *P < .05, **P < .01 (2-tailed Student t test). N.S., not significant.

Acknowledgments

The authors thank H. Miyoshi (RIKEN BioResource Center) for kindly providing lentivirus vectors encoding CSII-EF-MCS-IRES2-Venus, CSII-EF-MCS-IRES2-hKO1, and CSIV-TRE-Ubc-KT.

This research was supported by the Platform Project for Supporting Drug Discovery and Life Science Research (Basis for Supporting Innovative Drug Discovery and Life Science Research) and the Basic Science and Platform Technology Program for Innovative Biological Medicine from the Japan Agency for Medical Research and Development. This work was also supported by a KAKENHI Grant-in-Aid for Scientific Research (JSPS KAKENHI grants JP17H03597 and JP16K14632).

Authorship

Contribution: K.M. designed research, performed experiments, analyzed data, and wrote the manuscript; C.T. performed

experiments and analyzed data; S.M., H.K., M.N., A.I., M.Y., M.H., G.K., J.T., and T.R.K. helped collect data; T.B. and H.S. synthesized and designed the PI polyamides; T.N. and S.A. participated in discussions and interpretation of the data and results and commented on research direction; and Y.K. initiated and designed the study, supervised research, and gave the final approval for submission.

Conflict-of-interest disclosure: The authors declare no competing financial interests.

Correspondence: Yasuhiko Kamikubo, Department of Human Health Sciences, Graduate School of Medicine, Kyoto University, 53 Kawahara-cho, Syogoin, Sakyo-ku, Kyoto 606-8507, Japan; e-mail: kamikubo.yasuhiko.7u@kyoto-u.ac.jp; and Hiroshi Sugiyama, Department of Chemistry, Graduate School of Science, Kyoto University, Kitashirakawa-Oiwakecho, Sakyo-ku, Kyoto 606-8502, Japan; e-mail: hs@kuchem.kyoto-u.ac.jp.

References

1. Ben-Ami O, Friedman D, Leshkowitz D, et al. Addiction of t(8;21) and inv(16) acute myeloid leukemia to native RUNX1. *Cell Rep.* 2013;4(6):1131-1143.
2. Cunningham L, Finckbeiner S, Hyde RK, et al. Identification of benzodiazepine Ro5-3335 as an inhibitor of CBF leukemia through quantitative high throughput screen against RUNX1-CBF β interaction. *Proc Natl Acad Sci USA.* 2012;109(36):14592-14597.
3. Goyama S, Schibler J, Cunningham L, et al. Transcription factor RUNX1 promotes survival of acute myeloid leukemia cells. *J Clin Invest.* 2013;123(9):3876-3888.
4. Hyde RK, Kamikubo Y, Anderson S, et al. Cbfb/Runx1 repression-independent blockage of differentiation and accumulation of Csf2rb-expressing cells by Cbfb-MYH11. *Blood.* 2010;115(7):1433-1443.
5. Hyde RK, Zhao L, Alemu L, Liu PP. Runx1 is required for hematopoietic defects and leukemogenesis in Cbfb-MYH11 knock-in mice. *Leukemia.* 2015;29(8):1771-1778.
6. Morita K, Suzuki K, Maeda S, et al. Genetic regulation of the RUNX transcription factor family has antitumor effects. *J Clin Invest.* 2017;127(7):2815-2828.
7. Plaks V, Kong N, Werb Z. The cancer stem cell niche: how essential is the niche in regulating stemness of tumor cells? *Cell Stem Cell.* 2015;16(3):225-238.
8. Calvi LM, Adams GB, Weibrecht KW, et al. Osteoblastic cells regulate the haematopoietic stem cell niche. *Nature.* 2003;425(6960):841-846.
9. Kiel MJ, Yilmaz OH, Iwashita T, Yilmaz OH, Terhorst C, Morrison SJ. SLAM family receptors distinguish hematopoietic stem and progenitor cells and reveal endothelial niches for stem cells. *Cell.* 2005;121(7):1109-1121.
10. Winkler IG, Barbier V, Nowlan B, et al. Vascular niche E-selectin regulates hematopoietic stem cell dormancy, self renewal and chemoresistance. *Nat Med.* 2012;18(11):1651-1657.
11. Chien S, Haq SU, Pawlus M, et al. Adhesion of acute myeloid leukemia blasts to E-selectin in the vascular niche enhances their survival by mechanisms such as Wnt activation. *Blood.* 2013;122(21):61.
12. Ingrid G, Winkler VB, Ward M, et al. Vascular E-selectin protects leukemia cells from chemotherapy by directly activating pro-survival NF- κ B signaling: therapeutic blockade of E-selectin dampens NF- κ B activation. *Blood.* 2016;128(22):2823.
13. Morita K, Masamoto Y, Kataoka K, et al. BAALC potentiates oncogenic ERK pathway through interactions with MEK1 and KLF4. *Leukemia.* 2015;29(11):2248-2256.
14. Jiang CG, Li JB, Liu FR, Wu T, Yu M, Xu HM. Andrographolide inhibits the adhesion of gastric cancer cells to endothelial cells by blocking E-selectin expression. *Anticancer Res.* 2007;27(4B):2439-2447.
15. Zhu GD, Arendsen DL, Gunawardana IW, et al. Selective inhibition of ICAM-1 and E-selectin expression in human endothelial cells. 2. Aryl modifications of 4-(aryloxy)thieno[2,3-c]pyridines with fine-tuning at C-2 carbamides. *J Med Chem.* 2001;44(21):3469-3487.